ICASSP 2024 - 2024 IEEE International Conference on Acoustics, Speech and Signal Processing (ICASSP) | 979-8-3503-4485-1/24/$31.00 ©2024 IEEE | DOI: 10.1109/ICASSP48485.2024.10446005

CAMERA CALIBRATION USING A SINGLE VIEW OF A SYMMETRIC OBJECT

Hui Zhang[1⋆], *Bingran Kuang*[⋆], *Yajie Zhao*[†]

[⋆]Faculty of Science and Technology, United International College, BNU-HKBU, Zhuhai, P.R. China
[†]Institute for Creative Technologies, University of Southern California.

ABSTRACT

This paper addresses the problem of camera calibration and shape recovery using a single image of a reflectively symmetric object. Unlike existing methods requiring knowledge of 3D points or two images, this paper proposes to calibrate camera parameters using one image with known point distance ratios on 3D object. Specifically, we first recover the vanishing point of the symmetry plane normal. Then a set of candidate focal lengths are uniformly selected as the initial values, from which the pan and yaw angles of the camera can be obtained. To recover 3D points on the object, we recover the ratio of depth scale factors between symmetric 2D point pairs, then the ratio of depth scale factors between different symmetric points. Finally, constraints from 3D distance ratios on the object are used to refine the estimation of camera parameters. Both synthetic and real experiments demonstrate the feasibility of our method.

Index Terms— Camera calibration, symmetric object, mirror, single view, vanishing point.

1. INTRODUCTION

Camera Calibration plays an important role in 3D computer vision applications. Traditional methods restore camera parameters by capturing multiple images of a planar grid [25, 10, 9], which involves tedious manual works. Calibration with less preprocessing becomes a practical demand. To achieve this goal, researchers have proposed calibration methods under constrained motion, such as planar motion [11], pure rotation [19], turntable motion [23], and even general motion [13]. In addition, properties of object shapes are also explored, such as symmetry [8, 2], rotation invariance on surfaces of revolution (SOR) [20] or spheres [24].

Among them, the methods of using symmetry in [17, 15, 1, 12] describe how to calibrate camera extrinsics. Cao and Foroosh [5, 2] present methods for calibrating intrinsics. However, their works rely on an invariant cross ratio between four corresponding points of at least two images, which cannot be obtained when only one image is available. Wong et.al. [20] describes camera calibration using a imaged SOR. However, the rotational symmetry exhibited in SOR is different from the reflective symmetry [8] in symmetric objects. Vanishing point is also an important clue for camera calibration. Caprile and Torre [3], Hong et.al. [8] and Feng et.al.[4] present methods that can calibrate cameras from a single image. However, they require knowledge of at least two orthogonal vanishing points, which is difficult to obtain from a single image of a normally symmetric object. Martins et.al. [14] uses a single snapshot to calibrate camera intrinsics of mirror-reflected objects, but they require knowledge of at least 6 3D points. Works in [22, 16, 21] introduce methods using feature points or contours of objects in mirror images. However, they require at least two mirrors, i.e., two point sets of symmetrical reflections, to calibrate the camera and recover the object shape.

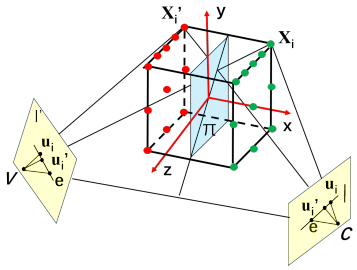

Fig. 1. A symmetric object with its symmetric plane.

Different from the above methods, this paper proposes a method that uses a single snapshot of a symmetric object to obtain intrinsic and extrinsic parameters and restore the 3D shape. The only pre-required knowledge is the 3D distance ratio on the object. Note that the distance ratio depends on the combination of distances, which introduces more constraints than using the coordinates of the 3D points directly. This is why our method is feasible when only a limited number of matching feature point pairs are available. Specifically, we first compute the fundamental matrix between real and virtual cameras that capture pairs of symmetric feature points in a 2D image, and from its eigenvector, we obtain the vanishing points of the normal for the symmetric plane. Then, we uniformly sample a set of candidate focal lengths from a given range and use our constraints to obtain two rotation angles, pan and yaw. To recover the 3D shape of the object, the ratio of depth scale factors between pairs of symmetric 2D points

[1]Corresponding author.

are obtained from the vanishing point. Meanwhile, using the constraints provided by the symmetric midpoint, we can obtain the ratio of the depth scale factors of each point. These will produce reconstructed 3D object points. Finally, refined camera intrinsic parameters are obtained during optimization by using constraints of known 3D distance ratios.

In summary, our contribution can be listed as follows. 1) We propose a novel method capable of calibrating camera intrinsics from a single view of a symmetric object without knowing positions of 3D object points. 2) We also propose a new method to calculate the depth scaling factor of each 3D point, which can help reconstruct the 3D shape of the object. 3) Using only a few feature points, the experimental results demonstrate the accuracy of our method.

2. PRELIMINARIES

A 3D point $\mathbf{X}_i = [x_i\ y_i\ z_i\ 1]^T$ $(i = 1, .., n)$ can be projected to its 2D image $\mathbf{u}_i = [u_i\ v_i\ 1]^T$ by a pinhole camera [7] as

$$\gamma_i[u_i\ \ v_i\ \ 1]^T = \mathbf{K}[\mathbf{R}|\mathbf{T}][x_i\ y_i\ z_i\ 1]^T, \tag{1}$$

where γ_i is a depth scale factor, $\mathbf{R}$ is a rotation matrix, and $\mathbf{T} = [t_x\ t_y\ t_z]^T$ is a translation vector. $\mathbf{K}$ is the intrinsics [7]

$$\mathbf{K} = \begin{bmatrix} \alpha f & s & u_0 \\ 0 & f & v_0 \\ 0 & 0 & 1 \end{bmatrix}, \tag{2}$$

where f is the focal length along the y-axis, α is the aspect ratio, $s = 0$ is the skew, and (u_0, v_0) is the principal point.

For a symmetric object, we assume that the yz-plane is the symmetric plane and x-axis aligns with its normal (see Fig. 1). A similar setup can be obtained when the symmetry plane is the xy or xz-plane. Here $\mathbf{X}_i$ is mapped to its symmetric point $\mathbf{X}'_i = [-x_i\ y_i\ z_i\ 1]^T$ by the matrix $\mathbf{M} = diag\{-1, 1, 1, 1\}$ and then projected onto its 2D image

$$\gamma'_i\mathbf{u}'_i = \gamma'_i[u'_i\ \ v'_i\ \ 1]^T = \mathbf{K}[\mathbf{R}|\mathbf{T}]\mathbf{M}[x_i\ y_i\ z_i\ 1]^T, \tag{3}$$

where γ'_i is a scale factor and the ratio λ_i between γ'_i and γ_i is

$$\lambda_i = \gamma'_i/\gamma_i. \tag{4}$$

Suppose $\mathbf{X}_i$ is projected to $\mathbf{u}'_i$ through virtual camera V, then the projection matrix is $\mathbf{P}' = \mathbf{K}[\mathbf{R}|\mathbf{T}]\mathbf{M}$. Therefore, the relationship between real camera C and V can be described as two camera view geometry, formulated with the fundamental matrix $\mathbf{F}$ [6], i.e., $\mathbf{u}'^T_i\mathbf{F}\mathbf{u}_i = 0$. Since C and V are symmetrical as shown in Fig. 1, $\mathbf{F}$ simplifies as [6]

$$\mathbf{F} = \begin{bmatrix} 0 & -1 & e_2 \\ 1 & 0 & -e_1 \\ -e_2 & e_1 & 0 \end{bmatrix}, \tag{5}$$

where $\mathbf{e} = \mathbf{e}' = [e_1\ e_2\ 1]^T$ is the epipole between C and V. Since $\mathbf{F}$ has a DoF of 2, $\mathbf{F}$ can be restored from at least two pairs of symmetric points, thereby recovering $\mathbf{e}$. From Fig. 1, it is easy to find that the vanishing point $\mathbf{v}_x$ of the normal for the symmetric plane is equal to $\mathbf{e}$, i.e., $\mathbf{v}_x = [e_1\ \ e_2\ \ 1]^T$.

3. RECOVERY OF THE ROTATION ANGLES

Given $\mathbf{v}_x$ which is also the vanishing point of the x-axis, the rotation matrix $\mathbf{R}$ can be partially recovered. Note that any rotation matrix can be obtained by multiplying the three basic rotation matrices around the x, y and z axes, as [18]

$$\begin{aligned}\mathbf{R} &= \mathbf{R}_z(\theta)\mathbf{R}_y(\phi)\mathbf{R}_x(\psi) \\ &= \begin{bmatrix} \cos\theta\cos\phi & \cos\theta\sin\phi\sin\psi - \sin\theta\cos\psi & \cos\theta\sin\phi\cos\psi + \sin\theta\sin\psi \\ \sin\theta\cos\phi & \sin\theta\sin\phi\sin\psi + \cos\theta\cos\psi & \sin\theta\sin\phi\cos\psi - \cos\theta\sin\psi \\ -\sin\phi & \cos\phi\sin\psi & \cos\phi\cos\psi \end{bmatrix},\end{aligned} \tag{6}$$

where the yaw θ, the pan ϕ and the tilt angle ψ are the rotation angles around z, y, x-axis, respectively.

Meanwhile, let γ_v be a non-zero scalar and the unit vector $\mathbf{r}_1$ be the 1st column of $\mathbf{R}$ in (6), $\mathbf{v}_x$ can be expressed as

$$\gamma_v\mathbf{v}_x = \mathbf{K}[\mathbf{R}|\mathbf{T}][1\ \ 0\ \ 0\ \ 0]^T = \mathbf{K}\mathbf{r}_1. \tag{7}$$

Suppose that the intrinsic matrix $\mathbf{K}$ is given, the scalar γ_v and the unit vector $\mathbf{r}_1 = [r_1\ r_2\ r_3]^T$ can be easily derived from

$$[r_1\ \ r_2\ \ r_3]^T = \gamma_v\mathbf{K}^{-1}\mathbf{v}_x. \tag{8}$$

The rotation angles θ and ϕ around the z and y axis can thus be calculated from $\mathbf{r}_1$, as

$$\theta = \arctan(r_2/r_1) \quad and \quad \phi = \arcsin(-r_3). \tag{9}$$

Now the only unrecovered parameter in $\mathbf{R}$ is ψ. However, ψ is not a necessary parameter to reconstruct the structure of the 3D object.

4. RECOVERY OF 3D STRUCTURE

To recover the structure of the 3D object, we first solve for the ratio λ_i between the depth scale factors γ_i and γ'_i of a pair of symmetric points $\mathbf{u}_i$ and $\mathbf{u}'_i$. We then find the ratios between depth scale factors of different feature points.

4.1. Ratio of Scalar Factors Between $\mathbf{u}_i$ and $\mathbf{u}'_i$

Note that by subtracting (1) from (3), we can derive the vanishing point $\mathbf{v}_x$ along the x-axis

$$\gamma_i(\mathbf{u}_i - \lambda_i\mathbf{u}'_i) = \mathbf{K}[\mathbf{R}|\mathbf{T}][2x_i\ \ 0\ \ 0\ \ 0]^T = 2x_i\gamma_v\mathbf{v}_x. \tag{10}$$

Let $\mathbf{v}_x = [v_x\ v_y\ 1]^T$, the ratio λ_i between γ_i and γ'_i is thus

$$\lambda_i = (u_i - v_x)/(u'_i - v_x). \tag{11}$$

4.2. Ratios Between Scale Factors at Different Points

Let $\mathbf{R}_{zy} = \mathbf{R}_z(\theta)\mathbf{R}_y(\phi)$, by adding (1) to (3), we can get

$$\gamma_i(\mathbf{u}_i + \lambda_i\mathbf{u}'_i) = \mathbf{K}\mathbf{R}_{zy}(2\mathbf{R}_x(\psi)\begin{bmatrix} 0 \\ y_i \\ z_i \end{bmatrix} + 2\mathbf{R}_{zy}^{-1}\begin{bmatrix} t_x \\ t_y \\ t_z \end{bmatrix}). \tag{12}$$

Let $\hat{\mathbf{X}}_i=[x_i\ \hat{y}_i\ \hat{z}_i]^T=\mathbf{R}_x(\psi)[x_i\ y_i\ z_i]^T$ be the 3D points after transforming $\mathbf{X}_i$ by $\mathbf{R}_x(\psi)$, $\hat{\mathbf{T}}=[\hat{t}_x\ \hat{t}_y\ \hat{t}_z]^T=\mathbf{R}_{zy}^{-1}[t_x\ t_y\ t_z]^T$ be the translation vector after transforming $\mathbf{T}$ with $\mathbf{R}_{zy}^{-1}$. Thus,

$$\begin{bmatrix}\hat{t}_x\\ \hat{t}_y\\ \hat{t}_z\end{bmatrix} = \frac{\gamma_i}{2}(\mathbf{K}\mathbf{R}_{zy})^{-1}(\mathbf{u}_i+\lambda_i\mathbf{u}_i')-\begin{bmatrix}0\\ \hat{y}_i\\ \hat{z}_i\end{bmatrix} = \gamma_i\begin{bmatrix}p_{ix}\\ p_{iy}\\ p_{iz}\end{bmatrix}-\begin{bmatrix}0\\ \hat{y}_i\\ \hat{z}_i\end{bmatrix}, \tag{13}$$

where $[p_{ix}\ p_{iy}\ p_{iz}]^T = (\mathbf{K}\mathbf{R}_{zy})^{-1}(\mathbf{u}_i + \lambda_i\mathbf{u}_i')/2$. Therefore,

$$\hat{t}_x = \gamma_i p_{ix}. \tag{14}$$

Note that the reconstructed 3D shape is invariant to $\hat{\mathbf{T}}$. Thus without loss of generality, for all symmetric point pairs $\mathbf{u}_i$ and $\mathbf{u}_i'$ $(i = 1, ..., n)$, the ratios $\beta_i = \gamma_i/\gamma_1$ between all γ_i and γ_1 of $\mathbf{u}_1$ can be calculated from $\gamma_i p_{ix} = \gamma_1 p_{1x}$, as

$$\beta_i = p_{1x}/p_{ix}. \tag{15}$$

4.3. Recovery of the 3D Points

From the obtained ratio β_i, the parameter along x-axis $\hat{t}_x$ of $\hat{\mathbf{T}}$ can be recovered up to the scalar γ_1. Meanwhile, since translation is a rigid body transformation, the shape of the 3D object will not be affected by the remaining 2 parameters (i.e., $\hat{t}_y$ and $\hat{t}_z$) in $\hat{\mathbf{T}}$. Now by substituting the obtained parameters in (1), we can recover 3D points $\tilde{\mathbf{X}}_i$ up to the scalar γ_1, by

$$\tilde{\mathbf{X}}_i = \hat{\mathbf{X}}_i + \hat{\mathbf{T}} = \gamma_1\beta_i(\mathbf{K}\mathbf{R}_{zy})^{-1}\mathbf{u}_i. \tag{16}$$

Note that the object of $\tilde{\mathbf{X}}_i$ shares the same structure as the original object of $\mathbf{X}_i$. The differences are the overall scalar γ_1, the rigid transformation introduced by $\mathbf{R}_x(\psi)$ and $\hat{\mathbf{T}}$.

5. CAMERA CALIBRATION

From the above, given the initial $\mathbf{K}$, the 3D points $\tilde{\mathbf{X}}_i$ can be recovered. In turn, we need some 3D priors as constraints to obtain optimal $\mathbf{K}$, such as the distance ratio. Let N be the number of points, given the initial $\mathbf{K}$, we can use the difference between the distance ratios of two points on the reconstructed object and the original object as the cost function,

$$cost = \sum_{i,j,k,q=1}^{N} |\frac{d(\tilde{\mathbf{X}}_i, \tilde{\mathbf{X}}_j)}{d(\tilde{\mathbf{X}}_k, \tilde{\mathbf{X}}_q)} - \frac{d(\mathbf{X}_i, \mathbf{X}_j)}{d(\mathbf{X}_k, \mathbf{X}_q)}|, \tag{17}$$

Let the distance between two points $\mathbf{X}_i$ and $\mathbf{X}_j$ be $d(\mathbf{X}_i, \mathbf{X}_j)$, i, j, k, q are indices of the four feature points and $i \neq j$, $k \neq q$. $|\cdot|$ is the absolute value. Levenberg–Marquardt algorithm is used to optimize the cost function, so as to get the optimal $\tilde{\mathbf{K}}$. Note that given a distance ratio, only f can be obtained. To estimate α as well, at least two non-coplanar distance ratios need to be known. Here the coplanar distance ratios provide dependency constraints, which do not help to obtain additional camera parameters. Similarly, to recover more parameters such as (u_0, v_0), at least four non-coplanar distance ratios need to be known.

6. EXPERIMENTS AND RESULTS

6.1. Synthetic Experiments

A cube of edge length 2 is generated as the symmetric object. Its half-cube consists of 11 3D points on a plane (red in Fig. 1) which is reflected to the symmetric positions (green) using the reflection plane $[1\ 0\ 0]^T$ (the colored plane). The 22 points are projected onto an image of size of 640×480. The GT camera parameters are $f = 855$, $\alpha = 1.05$, $s = 0.0$, and $(u_0, v_0) = (320, 240)$. The rotation angles and the translation vector are arbitrarily chosen as $-10^o, 20^o, 25^o$ and $(1, -1, -8)^T$, respectively. The initial focal lengths are selected from the range $[100, 2000]$ with a step size of 100, which are fed into an iterative process to find the optimal solution of $\mathbf{K}$. We added zero-mean Gaussian noise from 0.0 to 3.0 pixels with a step size of 0.1, to the projected 2D points and performed 100 independent experiments at each noise level.

Calibration given 2 distance ratios. Given at least two 3D point distance ratios, we can obtain f and α. At the noise level of 1.0, Fig. 2 (a)-(c) show the residual σ of the cost function, the optimized f and α under each initial $\hat{f}$. It can be seen that larger absolute values of σ indicate possible local minima. Therefore, we ignore the results when $|\sigma| \geq 10^{-7}$. Then for the remaining results, the third row of Table 1 (a) shows median and relative error of the result for f and α by selecting α close to 1. The third row of Table 1 (b) shows the corresponding rotation angles and 3D distance ratios, which demonstrates the accuracy of our method. Fig. 2 (d)-(h) illustrates the boxplots of the recovered f, α, θ, ϕ and 3D reconstruction errors under noise levels from 0.0 to 3.0.

Calibration given at least 4 distance ratios. In this experiment, the ground-truth offset $(\Delta u_0, \Delta v_0)$ of the principle point is set to $(5, -5)$, and other parameters are set as same as above. We can obtain four camera parameters. We use the minimum sum of the absolute values of the offset $|\Delta u_0| + |\Delta v_0|$ to select estimates of f and α. At the noise level of 1.0, the fourth rows of Table 1 (a) and (b) show the median and relative errors of the camera intrinsics, relative errors of θ, ϕ and the 3D distance ratio, respectively. These all prove the feasibility of our method. In practice, using four ratios becomes unstable when the noise level is greater than 1.0. These may due to the inaccuracy in 2D feature points. Therefore, 8 distances for 28 ratios are used to provide a more stable solution. Note that our method cannot be applied when the vanishing point $\mathbf{v}_x$ is at infinity when the image plane is orthogonal to the object symmetry plane. Meanwhile, the method cannot be applied when self-occlusion makes one side of the feature point invisible to the camera.

6.2. Real Experiments

In real experiment, ground-truth camera parameters are obtained using Zhang's method [25]. A picture (see Fig. 3 (a)) of a cabinet is then taken with a Nikon D30 camera with an

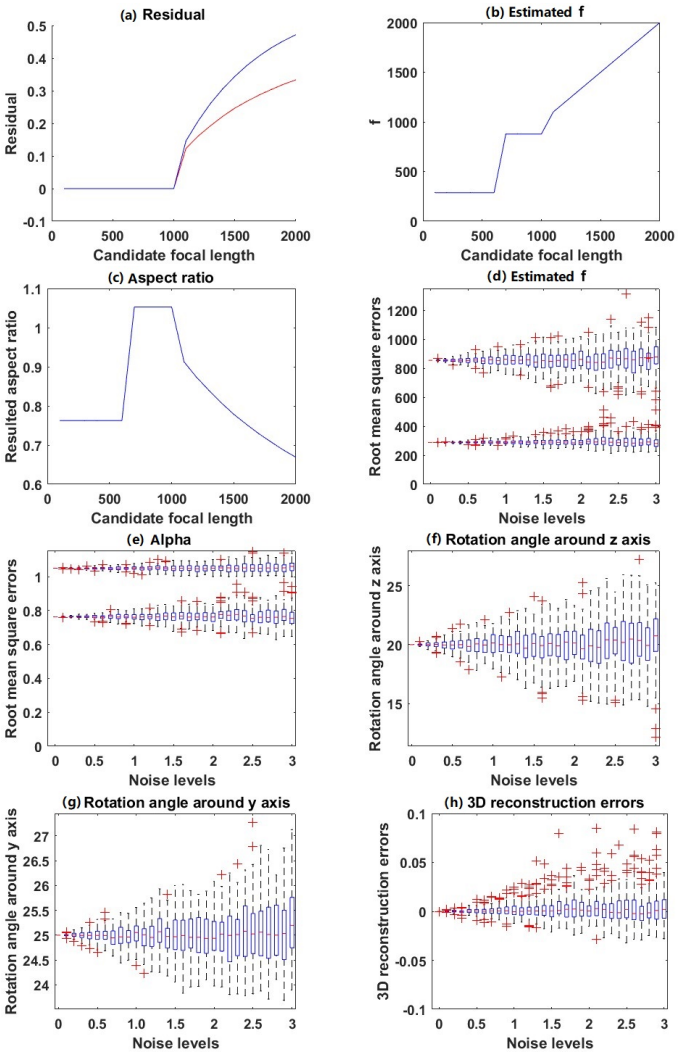

Fig. 2. Known 2 distance ratios, (a)-(c) show results given different initial focal lengths under the noise level 1.0. (d)-(h) Boxplots of the results under noise levels from 0 to 3.0.

Table 1. Known 2, 4 distance ratios, results of calibrating intrinsic parameters, two rotation angles and the 3D distance ratios at the noise level of 1.0.

-	f	α	$w/2+\Delta u_0$	$h/2+\Delta v_0$
GT	855	1.05	320+5	240-5
2 ratios	**854.87 (0.02%)**	**1.048 (0.19%)**	-	-
4 ratios	857.20 (0.26%)	1.05 (0.00%)	320+16.09 (3.40%)	240+0.08 (2.16%)

(a) Results of camera intrinsics.

-	θ	ϕ	3D distance ratio
GT	25	20	2
2 ratios	24.09 (0.20%)	19.97 (0.15%)	2 ± 0.005(0.26%)
4 ratios	25.07 (0.28%)	19.98 (0.10%)	2 ± 0.01 (0.50%)

(b) Recovered rotation angles and mean of 3D distance ratios.

image resolution of 3120×2080. Following the way in [2], we manually selected 18 pairs of symmetric points with the Matlab control point selection tool. Using 2 or 28 known distance ratios, our method can calibrate 2 camera external, and 2 or 4 internal parameters, respectively. According to the obtained values of cost residuals, we ignore the results when $|\sigma| \geq 10^{-1}$. Table 2 shows the calibrated intrinsics, the calibrated angles and 3D reconstruction errors, respectively. Errors could be reduced by increasing the number of symmetric points. Figure 3 (b) shows the reconstructed 3D model. It can be seen that our method is practical and can be applied to 3D reconstruction with high accuracy.

(a) A picture of a cabinet. (b) The reconstructed model.

Fig. 3. Real experiments.

Table 2. Results of calibrating 2, 4 camera intrinsics, using 2, 28 distance ratios, respectively.

-	f	α	$w/2+\Delta u_0$	$h/2+\Delta v_0$
GT	2381.66	1.0010	1542.92	1004.65
2 ratios	2451.67 (2.94%)	1.0135 (1.25%)	-	-
28 ratios	2343.58 (1.69%)	1.0068 (0.58%)	1441.17 (6.60%)	906.29 (9.80%)

(a) f, α, u_0, v_0.

-	θ	ϕ	3D ratios
#1 GT	35.83	20.18	1.72
2 ratios	36.68 (2.38%)	20.88 (3.49%)	0.0308(1.79%)
28 ratios	36.79 (2.68%)	18.18 (8.89%)	0.0836(4.87%)

(b) Rotation angles and 3D distance ratios.

7. CONCLUSION

This paper presents a method to calibrate camera parameters and reconstruct 3D geometry using only a single image of a symmetric object. Our method is able to calibrate one, two or even four parameters of the camera with knowledge of distance ratios on the object. This is achieved by using our newly discovered constraints for recovering ratios of depth scale factors during an iterative optimization process. By increasing the number of known distance ratios, four camera intrinsics can be obtained. Both synthetic and real experiments demonstrate the feasibility of our method.

8. REFERENCES

[1] A. Agrawal, Extrinsic Camera Calibration Without a Direct View Using Spherical Mirror, in Proc. of International Conference on Computer Vision, 2368–2375, 2013.

[2] X. Cao and H. Foroosh, Camera Calibration Using Symmetric Objects, IEEE Trans on Image Processing, 15(11):3614-3619, Nov. 2006.

[3] B. Caprile and V. Torre, Using Vanishing Points for Camera Calibration, International Journal of Computer Vision (IJCV), 4:127–139, 1990.

[4] X. F. Feng and D. F. Pan, A Camera Calibration Method Based on Plane Mirror and Vanishing Point Constraint, Optik - International Journal for Light and Electron Optics, 558-565, 2017.

[5] H. Foroosh, M. Balci, and X. Cao, Self-Calibrated Reconstruction of Partially Viewed Symmetric Objects, in Proc. IEEE ICASSP, pp.869–872, 2005.

[6] S. Fujiyama, F. Sakaue, J, Sato, Multiple View Geometries for Mirrors and Cameras, in Proc. of International Conference on Pattern Recognition, 45–48, Istanbul, Turkey, 2010.

[7] R. Hartley and A. Zisserman. Multiple View Geometry in Computer Vision. Cambridge University Press, 2nd ed edition, 2004.

[8] W. Hong, A. Y. Yang, and Y. Ma. On Group Symmetry in Multiple View Geometry: Structure, Pose and Calibration From Single Images. IJCV, 60, pages 241–265, 2004.

[9] H. Huang, H. Zhang, and Y. M. Cheung. The Common Self-Polar Triangle of Concentric Circles and its Application to Camera Calibration, In Prof. of 2015 IEEE Conference on Computer Vision and Pattern Recognition (CVPR), 4065-4072, 2015.

[10] J. S. Kim, P. Gurdjos, and I. S. Kweon. Geometric and Algebraic Constraints of Projected Concentric Circles and Their Applications to Camera Calibration. IEEE Trans. on Pattern Analysis and Machine Intelligence, 27(4):637–642, 2005.

[11] J. Knight, A. Zisserman, I. Reid, Linear Auto-Calibration for Ground Plane Motion, in Prof. of IEEE Conference on Computer Vision and Pattern Recognition,503–510, Madison, USA, 2003

[12] R. K. Kumar, A. Ilie, J. M. Frahm and M. Pollefeys, Simple Calibration of Non-Overlapping Cameras With a Mirror, in Proc. of IEEE Conference on Computer Vision and Pattern Recognition, Anchorage, AK, USA, 2008.

[13] Y. Liu and H. Zhang, Camera Auto-Calibration From the Steiner Conic of the Fundamental Matrix, IEEE Conference on European Conference on Computer Vision, pp 431–446, November 2022.

[14] N. C. Martins and J. M. Dias, Camera Calibration Using Reflections in Planar Mirrors and Object Reconstruction Using Volume Carving Method, The Imaging Science Journal, 52(2):117-130, June 2004.

[15] K. Takahashi, S. Nobuhara, T. Matsuyama, A New Mirror-Based Extrinsic Camera Calibration Using an Orthogonality Constraint, in Proc. of IEEE Conference on Computer Vision and Pattern Recognition, Providence, 1051-1058, RI, USA, 2012.

[16] K. Takahashi, S. Nobuhara, Camera Calibration Based on Mirror Reflections, IPSJ SIG Technical Report, 2018.

[17] L. Kneip, X. Li, X. Zhang, Q. Yu and G. Long, Simplified Mirror-Based Camera Pose Computation via Rotation Averaging,in Proc. of IEEE Conference on Computer Vision and Pattern Recognition, 2015

[18] T. Herter and K. Lott, Algorithms for Decomposing 3D Orthogonal Matrices Into Primitive Rotations, Computers and Graphics, 17(5): 517–527, October 1993.

[19] L. Wang, S. B. Kang; H. Y. Shum and G. Xu, Error Analysis of Pure Rotation-Based Self-Calibration, In Proc. of IEEE International Conference on Computer Vision (ICCV), 275-280, Vancouver, Canada, 2001

[20] K.-Y. K. Wong, P. R. S. Mendonça and R. Cipolla. Camera Calibration from Surfaces of Revolution. IEEE Transactions on Pattern Analysis and Machine Intelligence (TPAMI), 25(2):147-161, February 2003.

[21] X. Ying, K. Peng, Y. Hou, S. Guan, J. Kong and H. Zha, Self-Calibration of Catadioptric Camera with Two Planar Mirrors from Silhouettes. IEEE Trans. Pattern Anal. Mach. Intell. 35(5): 1206-1220, 2013.

[22] H. Zhang, L. Shao and K.-Y. K. Wong. Self-calibration and Motion Recovery from Silhouettes with Two Mirrors. Asian Conference on Computer Vision (ACCV), volume 4, pages 1-12, Deajeon, Korea, November 2012.

[23] H. Zhang and K. Y. Wong. Self-Calibration of Turntable Sequences From Silhouettes. IEEE Transactions on Pattern Analysis and Machine Intelligence, 31:5–14, 2009.

[24] H. Zhang, K.-Y. K. Wong and G. Zhang. Camera Calibration From Images of Spheres. IEEE Transactions on Pattern Analysis and Machine Intelligence (TPAMI), 29(3):499-503, March 2007.

[25] Z. Zhang. A Flexible New Technique for Camera Calibration. IEEE Transactions on Pattern Analysis and Machine Intelligence, pages 1330–1334, 2000.